

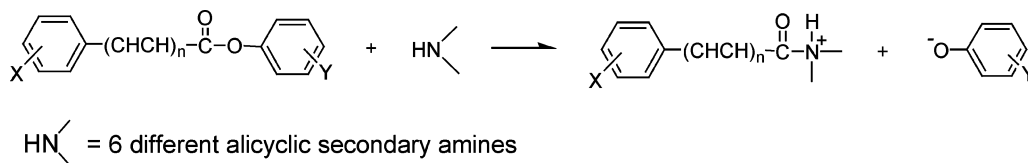
Aminolysis of Y-Substituted Phenyl X-Substituted Cinnamates and Benzoates: Effect of Modification of the Nonleaving Group from Benzoyl to Cinnamoyl

Ik-Hwan Um,^{*,‡} Youn-Min Park,[‡] Mizue Fujio,[†] Masaaki Mishima,[†] and Yuho Tsuno[†]

Division of Nano Sciences and Department of Chemistry, Ewha Womans University, Seoul 120-750, Korea, and Institute for Materials Chemistry and Engineering, Kyushu University, Hakozaki, Higashi-ku, Fukuoka 812-8581, Japan

ihum@ewha.ac.kr

Received March 11, 2007



A kinetic study is reported for reactions of Y-substituted phenyl X-substituted cinnamates (**1a–e** and **3a–g**) and benzoates (**2a–e** and **4a–g**) with a series of alicyclic secondary amines in 80 mol % H₂O/20 mol % DMSO at 25.0 ± 0.1 °C. Reactions of 2,4-dinitrophenyl X-substituted cinnamates (**1a–e**) and benzoates (**2a–e**) with amines result in linear Yukawa–Tsuno plots. The ρ_X values are much smaller for the reactions of **1a–e** than for those of **2a–e**. A distance effect and the nature of the reaction mechanism (i.e., a concerted mechanism for **1a–e**) have been suggested to be responsible for the small ρ_X values. The Brønsted-type plots for the reactions of 2,4-dinitrophenyl X-substituted cinnamates (**1a**, **1c**, and **1e**) with amines are curved with a decreasing β_{nuc} value from 0.65 to 0.3–0.4. The reactions of Y-substituted phenyl cinnamates (**3a–g**) with morpholine also result in a curved Brønsted plot, while the corresponding reactions of Y-substituted phenyl benzoates (**4a–e**) exhibit a linear Brønsted plot. It has been concluded that the curved Brønsted plots found for the reactions of the cinnamates (**1a**, **1c**, **1e**, and **3a–g**) are not due to a change in the rate-determining step (RDS) but due to a normal Hammond effect for a concerted mechanism, that is, an earlier transition state (TS) for a more reactive amine or substrate.

Introduction

There is continuous interest in acyl group transfer reactions due to the importance in biological processes as well as synthetic applications.^{1–10} Reactions of aryl acetates with aryloxides have been suggested to proceed through a concerted or stepwise

mechanism depending on the reaction conditions. Williams et al. have found a linear Brønsted-type plot for reactions of 4-nitrophenyl acetate with a series of substituted phenoxides

* To whom correspondence should be addressed. Tel: 82-2-3277-2349. Fax: 82-2-3277-2844.

[‡] Ewha Womans University.

[†] Kyushu University.

(1) (a) Jencks, W. P. *Chem. Rev.* **1985**, *85*, 511–527. (b) Castro, E. A. *Chem. Rev.* **1999**, *99*, 3505–3524. (c) Lee, I.; Sung, D. D. *Curr. Org. Chem.* **2004**, *8*, 557–567. (d) Page, M. I.; Williams, A. *Organic and Bio-organic Mechanisms*; Longman: Harlow, U.K., 1997; Chapter 7.

(2) (a) Williams, A. *Acc. Chem. Res.* **1989**, *22*, 387–392. (b) Ba-Saif, S.; Luthra, A. K.; Williams, A. *J. Am. Chem. Soc.* **1987**, *109*, 6362–6368. (c) Boume, N.; Chrystiuk, E.; Davis, A. M.; Williams, A. *J. Am. Chem. Soc.* **1988**, *110*, 1890–1895.

(3) (a) Buncel, E.; Um, I. H.; Hoz, S. *J. Am. Chem. Soc.* **1989**, *111*, 971–975. (b) Um, I. H.; Hwang, S. J.; Buncel, E. *J. Org. Chem.* **2006**, *71*, 915–920.

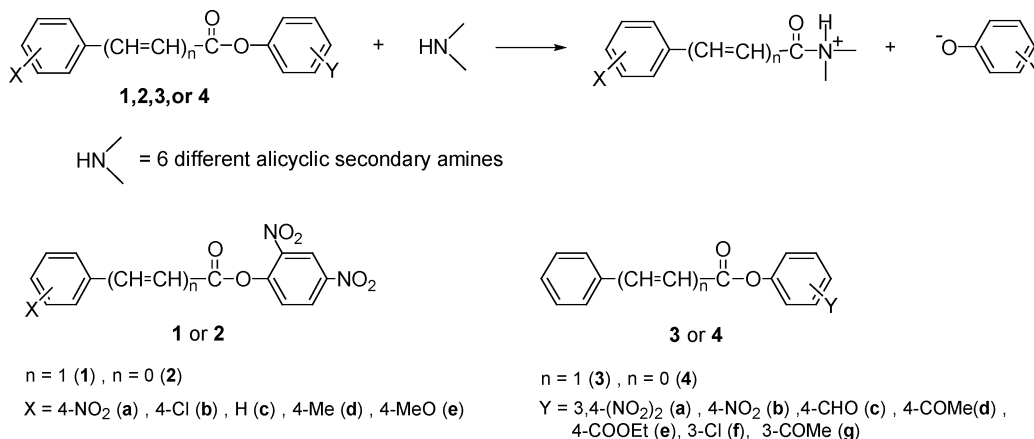
(4) (a) Sung, D. D.; Koo, I. S.; Yang, K.; Lee, I. *Chem. Phys. Lett.* **2006**, *426*, 280–284. (b) Sung, D. D.; Koo, I. S.; Yang, K.; Lee, I. *Chem. Phys. Lett.* **2006**, *432*, 426–430. (c) Oh, H. K.; Oh, J. Y.; Sung, D. D.; Lee, I. *J. Org. Chem.* **2005**, *70*, 5624–5629. (d) Oh, H. K.; Park, J. E.; Sung, D. D.; Lee, I. *J. Org. Chem.* **2004**, *69*, 9285–9288. (e) Oh, H. K.; Ha, J. S.; Sung, D. D.; Lee, I. *J. Org. Chem.* **2004**, *69*, 8219–8223. (f) Oh, H. K.; Park, J. E.; Sung, D. D.; Lee, I. *J. Org. Chem.* **2004**, *69*, 3150–3153.

(5) Gresser, M. J.; Jencks, W. P. *J. Am. Chem. Soc.* **1977**, *99*, 6970–6980.

(6) (a) Castro, E. A.; Santander, C. L. *J. Org. Chem.* **1985**, *50*, 3595–3600. (b) Castro, E. A.; Valdivia, J. L. *J. Org. Chem.* **1986**, *51*, 1668–1672. (c) Castro, E. A.; Steinfert, G. B. *J. Chem. Soc., Perkin Trans. 2* **1983**, 453–457.

(7) (a) Castro, E. A.; Aguayo, R.; Bessolo, J.; Santos, J. G. *J. Org. Chem.* **2005**, *70*, 778–7791. (b) Castro, E. A.; Aguayo, R.; Bessolo, J.; Santos, J. G. *J. Org. Chem.* **2005**, *70*, 3530–3536. (c) Castro, E. A.; Vivanco, M.; Aguayo, R.; Aguayo, R.; Santos, J. G. *J. Org. Chem.* **2004**, *69*, 5399–5404. (d) Castro, E. A.; Aguayo, R.; Santos, J. G. *J. Org. Chem.* **2003**, *68*, 8157–8161.

SCHEME 1



whose pK_a values straddle the basicity of the leaving 4-nitrophenoxide, and they concluded that the reactions proceed through a concerted mechanism.² On the contrary, Buncel et al. have suggested that reactions of substituted phenyl acetates with phenoxide proceed through an addition intermediate with its formation being the rate-determining step (RDS) on the basis of the fact that σ^o constants result in better Hammett correlation with rate constants than σ^- constants.³

Aminolyses of esters with a good leaving group have often resulted in a curved Brønsted-type plot, which has generally been interpreted as a change in the RDS.^{1,4–10} The RDS has been suggested to change at pK_a^o , defined as the pK_a at the center of the Brønsted curvature, from breakdown of a zwitterionic tetrahedral intermediate (T^\pm) to its formation as the amine basicity increases.^{1,4–10} An intriguing aspect is whether the pK_a^o value is influenced by the electronic nature of the substituent in the nonleaving group (i.e., the acyl moiety of esters) or not.

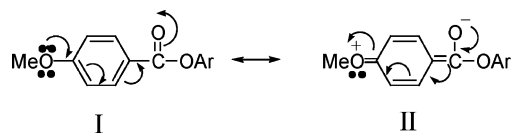
Gresser and Jencks have reported that the pK_a^o value increases as the substituent in the nonleaving group becomes a stronger electron-withdrawing group (EWG) for quinuclidinolysis of diaryl carbonates.⁵ This was explained through the argument that the departure of amine from T^\pm is favored over that of the leaving group, as the substituent in the nonleaving group becomes a stronger EWG.⁵ Castro et al. have found a similar result for pyridinolysis of 2,4-dinitrophenyl X-substituted benzoates (i.e., $pK_a^o = 9.5$ when X = H but $pK_a^o > 9.5$ when X = Cl, CN, NO₂)⁶ and (*S*)-2,4-dinitrophenyl X-substituted thiobenzoates (i.e., pK_a^o increases from 8.5 to 8.9 and 9.9 as X changes from 4-Me to H and 4-NO₂, respectively) in aqueous ethanol.⁷

In contrast, we have shown that the pK_a^o value does not vary on changing the electronic nature of the substituent X in the nonleaving group for aminolyses of 2,4-dinitrophenyl X-

substituted benzoates, benzenesulfonates, and related compounds in 80 mol % H₂O/20 mol % DMSO.^{8–11} We have found that the Hammett plots for these reactions are curved downwardly as the substituent in the nonleaving group changes from EWGs to electron-donating groups (EDGs). Traditionally, such a curved Hammett plot has been interpreted as a change in the RDS.¹² However, we have suggested that the nonlinear Hammett plots are not due to a change in the RDS since the Yukawa–Tsuno plots for the same reactions exhibit an excellent linearity with large r values.^{8–11} The r value in the Yukawa–Tsuno equation (eq 1) represents the resonance demand of the reaction center or the extent of resonance contribution.^{13,14} Thus, we have concluded that ground-state (GS) stabilization through resonance interactions as illustrated by the resonance structures I \leftrightarrow II is responsible for the nonlinear Hammett plots.^{8–11}

$$\log k^X/k^H = \rho_X[\sigma^o + r(\sigma^+ - \sigma^o)] \quad (1)$$

To obtain further information about the effect of a nonleaving



group on acyl transfer reactions, we have extended our study to reactions of Y-substituted phenyl X-substituted cinnamates (**1a–e** and **3a–g**) and benzoates (**2a–e** and **4a–g**) with a series of alicyclic secondary amines whose pK_a values range from 11.02 to 5.95 (Scheme 1). Modification of the nonleaving group

(11) Um, I. H.; Lee, E. J.; Seok, J. A.; Kim, K. H. *J. Org. Chem.* **2005**, *70*, 7530–7536.

(12) (a) Carrol, F. A. *Perspectives on Structure and Mechanism in Organic Chemistry*; Brooks/Cole: New York, 1998; pp 371–386. (b) Lowry, T. H.; Richardson, K. S. *Mechanism and Theory in Organic Chemistry*, 3rd ed.; Harper Collins Publishers: New York, 1987; pp 143–151. (c) Swansburg, S.; Buncel, E.; Lemieux, R. P. *J. Am. Chem. Soc.* **2000**, *122*, 6594–6600.

(13) (a) Tsuno, Y.; Fujio, M. *Adv. Phys. Org. Chem.* **1999**, *32*, 267–385. (b) Tsuno, Y.; Fujio, M. *Chem. Soc. Rev.* **1996**, *25*, 129–139. (c) Yukawa, Y.; Tsuno, Y. *Bull. Chem. Soc. Jpn.* **1959**, *32*, 965–970.

(14) (a) Fujio, M.; Umezaki, Y.; Alam, Md. A.; Kikukawa, K.; Fujiyama, R.; Tsuno, Y. *Bull. Chem. Soc. Jpn.* **2006**, *79*, 1091–1099. (b) Fujio, M.; Uchida, M.; Okada, A.; Alam, Md. A.; Fujiyama, R.; Siehl, H. U.; Tsuno, Y. *Bull. Chem. Soc. Jpn.* **2005**, *78*, 1834–1842. (c) Fujio, M.; Rappoport, Z.; Uddin, M. K.; Kim, H. J.; Tsuno, Y. *Bull. Chem. Soc. Jpn.* **2003**, *76*, 163–169. (d) Nakata, K.; Fujio, M.; Nishimoto, K.; Tsuno, Y. *J. Phys. Org. Chem.* **2003**, *16*, 323–335.

(8) (a) Um, I. H.; Hwang, S. J.; Baek, M. H.; Park, E. J. *J. Org. Chem.* **2006**, *71*, 9191–9197. (b) Um, I. H.; Lee, J. Y.; Ko, S. H.; Bae, S. K. *J. Org. Chem.* **2006**, *71*, 5800–5803. (c) Um, I. H.; Jeon, S. E.; Seok, J. A. *Chem.–Eur. J.* **2006**, *12*, 1237–1243. (d) Um, I. H.; Lee, J. Y.; Lee, H. W.; Nagano, Y.; Fujio, M.; Tsuno, Y. *J. Org. Chem.* **2005**, *70*, 4980–4987. (e) Um, I. H.; Kim, K. H.; Park, H. R.; Fujio, M.; Tsuno, Y. *J. Org. Chem.* **2004**, *69*, 3937–3942. (f) Um, I. H.; Min, J. S.; Ahn, J. A.; Hahn, H. J. *J. Org. Chem.* **2000**, *65*, 5659–5663.

(9) (a) Um, I. H.; Hong, J. Y.; Seok, J. A. *J. Org. Chem.* **2005**, *70*, 1438–1444. (b) Um, I. H.; Chun, S. M.; Chae, O. M.; Fujio, M.; Tsuno, Y. *J. Org. Chem.* **2004**, *69*, 3166–3172. (c) Um, I. H.; Hong, J. Y.; Kim, J. J.; Chae, O. M.; Bae, S. K. *J. Org. Chem.* **2003**, *68*, 5180–5185.

(10) (a) Um, I. H.; Lee, J. Y.; Fujio, M.; Tsuno, Y. *Org. Biomol. Chem.* **2006**, *4*, 2979–2985. (b) Um, I. H.; Lee, J. Y.; Kim, H. T.; Bae, S. K. *J. Org. Chem.* **2004**, *69*, 2436–2441. (c) Um, I. H.; Ahn, J. A.; Kang, S.; Buncel, E. *J. Org. Chem.* **2002**, *67*, 8475–8480.

TABLE 1. Summary of Second-Order Rate Constants for Reactions of 2,4-Dinitrophenyl X-Substituted Cinnamates (**1a–e**) (and Benzoates **2a–e**, in Parenthesis) with Alicyclic Secondary Amines in 80 mol % H₂O/20 mol % DMSO at 25.0 ± 0.1 °C^a

substituent	$k_N/M^{-1} s^{-1}$		
	piperidine	morpholine	piperazinium ion
a X = 4-NO ₂	640 (2880)	65.0 (138)	1.48 (1.83)
b X = 4-Cl	253 (371)	27.0 (32.7)	0.748 (0.675)
c X = H	193 (174)	22.7 (19.6)	0.707 (0.467)
d X = 4-CH ₃	140 (100)	15.8 (11.2)	0.501 (0.306)
e X = 4-CH ₃ O	92.5 (56.2)	10.6 (5.77)	0.354 (0.162)

^a The data in the parenthesis are the k_N values for the reactions of the benzoates **2a–e** taken from ref 8e.

from benzoyl to cinnamoyl should provide insights into the reactivity and the comparative reaction mechanism. We have probed the effect of changing the substrate from the benzoates (**2a–e** and **4a–g**) to the cinnamates (**1a–e** and **3a–g**) on the reactivity, the reaction mechanism, and, notably, the r value in their Yukawa–Tsuno plots and report the kinetic results herein.

Results and Discussion

All reactions in this study obeyed pseudo-first-order kinetics over 90% of the total reaction. Pseudo-first-order rate constants (k_{obsd}) were determined from the equation $\ln(A_{\infty} - A_t) = -k_{\text{obsd}}t + C$. The correlation coefficients for the linear regressions were usually higher than 0.9995. The plots of k_{obsd} versus amine concentration were linear, passing through the origin, indicating that general base catalysis by a second amine molecule is absent and the contribution of H₂O and/or OH⁻ from hydrolysis of amine to the k_{obsd} is negligible. Thus, the rate law is given by eq 2, in which [S] and [NH] represent the concentration of the substrate and amine, respectively. The second-order rate constants (k_N) were determined from the slopes of the linear plots of k_{obsd} versus amine concentration and are summarized in Tables 1–3.

The uncertainty in the k_N values is estimated to be less than 3% from replicate runs. The detailed reaction conditions and kinetic results are given in the Supporting Information.

$$\text{rate} = k_{\text{obsd}}[\text{S}], \text{ where } k_{\text{obsd}} = k_N[\text{NH}] \quad (2)$$

Effect of a Nonleaving Group Substituent on Reactivity, r , and Mechanism. As shown in Table 1, the reactivity of **1a–e** decreases as the substituent X in the cinnamoyl moiety changes from a strong EWG to an EDG. A similar result is shown in the parenthesis for the corresponding reactions of **2a–e**. Interestingly, the cinnamates with a strong electron-withdrawing substituent (i.e., **1a** and **1b**) are less reactive than the corresponding benzoates (i.e., **2a** and **2b**), while the cinnamates with an electron-donating substituent (i.e., **1c–e**) are more reactive than the corresponding benzoates (i.e., **2c–e**).

The effect of substituent X on reactivity is illustrated in panels A and B of Figure 1 for the reactions of **1a–e** and **2a–e**, respectively. The Yukawa–Tsuno plots for the reactions of **1a–e** exhibit good linear correlations. This contrasts the Hammett plots for the same reactions in which **1d** and **1e** exhibit negative deviations (Figure S1 in the Supporting Information). The linear Yukawa–Tsuno plots shown in Figure 1A indicate

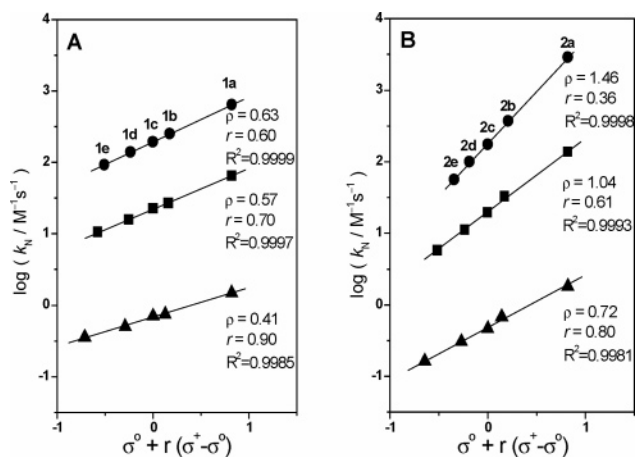
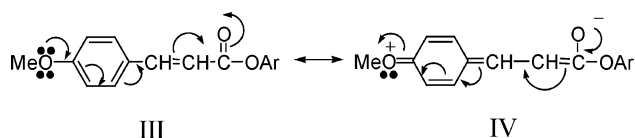


FIGURE 1. Yukawa–Tsuno plots for reactions of 2,4-dinitrophenyl X-substituted cinnamates (A) and benzoates (B) with piperidine (●), morpholine (■), and piperazinium ion (▲) in 80 mol % H₂O/20 mol % DMSO at 25.0 ± 0.1 °C. The identity of points is given in Table 1.

that the reactions proceed without changing the RDS or reaction mechanism on changing the substituent X in the cinnamoyl moiety. This result is consistent with our recent reports that the substituent in the nonleaving group does not influence the reaction mechanism for reactions of aryl-substituted benzoates and related compounds with various nucleophiles.^{8–11}

The Yukawa–Tsuno plots for the corresponding reactions of **2a–e** are also linear (Figure 1B). It is noted that the reactions of **1a–e** exhibit larger r values with much smaller ρ_X values than those of **2a–e**. The r in the Yukawa–Tsuno equation (eq 1) represents the resonance demand of the reaction center or the extent of resonance contribution.^{13,14} Since the r values are larger for the reactions of **1a–e** than for those of **2a–e**, the presence of the $-\text{CH}=\text{CH}-$ bond in the cinnamates **1a–e** increases the resonance contribution in the GS as illustrated in the resonance structures III ↔ IV.



Many factors have been suggested to influence the ρ_X value. These include the charge type and the basicity of nucleophiles, the distance from the reaction site to the substituent, and the nature of reaction mechanism in a given reaction medium.^{8,10a,15–19} Reactions with anionic nucleophiles have been reported to exhibit larger ρ_X values than for those with neutral amines.^{10a} For reactions with neutral amines, the more basic amine exhibits a larger ρ_X value than the less basic one.⁸ In fact, in the current study, the ρ_X value decreases from 0.63 to 0.41 and 1.46 to 0.72 for the reactions of **1a–e** and **2a–e**, respectively, as the amine changes from strongly basic piperidine to a weakly basic

(15) Carrol, F. A. *Perspectives on Structures and Mechanism in Organic Chemistry*; Brooks/Cole: New York, 1998; pp 371–380.

(16) Jencks, W. P. *Catalysis in Chemistry and Enzymology*; McGraw-Hill: New York, 1969; pp 480–483.

(17) (a) Menger, F. M.; Smith, J. H. *J. Am. Chem. Soc.* **1972**, *94*, 3824–3829. (b) Kim, T. H.; Huh, C.; Lee, B. S.; Lee, I. *J. Chem. Soc. Perkin Trans. 2* **1995**, 2257–2261.

(18) (a) Jaffe, H. H. *Chem. Rev.* **1953**, *53*, 191–261. (b) O’Ferrall, R. M.; Miller, S. I. *J. Am. Chem. Soc.* **1963**, *85*, 2440–2444.

(19) Hansch, C.; Leo, A.; Taft, R. W. *Chem. Rev.* **1991**, *91*, 165–195.

TABLE 2. Summary of Second-Order Rate Constants for Reactions of 2,4-Dinitrophenyl X-Substituted Cinnamates **1a** (X = 4-NO₂), **1c** (X = H), and **1e** (X = 4-MeO) with Alicyclic Secondary Amines in 80 mol % H₂O/20 mol % DMSO at 25.0 ± 0.1 °C

amine	pK _a	k _N /M ⁻¹ s ⁻¹		
		1a	1c	1e
1 piperidine	11.02	640	193	92.5
2 3-methyl piperidine	10.8	621	186	83.8
3 piperazine	9.85	264	115	50.7
4 morpholine	8.65	65.0	22.7	10.6
5 1-formyl piperazine	7.98	20.7	7.37	3.46
6 piperazinium ion	5.95	1.48	0.707	0.354

piperazinium ion. It has also been reported that insertion of one -CH₂- or -CH=CH- group between the reaction site and the substituent causes a decrease in ρ_X by a half.^{15,18} One can see from Figure 1A and 1B that the ρ_X values for the reactions of **1a–e** are about one-half of those for the corresponding reactions of **2a–e**. Accordingly, one might attribute the small ρ_X values found for the reactions of **1a–e** to a distance effect due to the presence of the -CH=CH- bond between the reaction site and the substituent.

However, if the distance effect is solely responsible for the small ρ_X values obtained for the reactions of **1a–e**, the ρ_X(**1a–e**)/ρ_X(**2a–e**) ratio should be independent of the basicity of the amines studied. One can calculate from Figure 1A and 1B that the ρ_X(**1a–e**)/ρ_X(**2a–e**) ratio increases from 0.43 to 0.55 and 0.57 as the amine changes from piperidine to morpholine and piperazinium ion, respectively. The dependence of the ρ_X(**1a–e**)/ρ_X(**2a–e**) ratio on the basicity of amines suggests that the distance effect is not solely responsible for the small ρ_X values. One can suggest that the nature of reaction mechanism (i.e., a concerted mechanism for the reaction of **1a–e**) might be another cause for the small ρ_X value since reactions which proceed through a concerted mechanism often result in a small ρ_X value.^{15–19} However, the present ρ_X value alone cannot provide any conclusive information on the reaction mechanism.

Effect of Amine Basicity on Reactivity and Mechanism.

As shown in Table 2, the reactivity of amines toward the cinnamates **1a**, **1c**, and **1e** decreases as the basicity of amines decreases. The effect of amine basicity on reactivity is illustrated in Figure 2. The Brønsted-type plots for the reactions of **1a**, **1c**, and **1e** with the six amines are curved when the pK_a and k_N values were statistically corrected using *p* and *q*.²⁰

A downward curvature in Brønsted-type plots has generally been interpreted as a change in the RDS or in the TS structures depending on the degree of the curvature.^{1,4–10} Aminolysis of esters with a good leaving group has often been reported to result in a curved Brønsted-type plot; that is, β_{nuc} decreases from 0.8–1.0 to 0.1–0.3 as the amine becomes more basic than the leaving group by 4–5 pK_a units.^{1,4–10} Such a large change in β_{nuc} values has been suggested as a change in the RDS from breakdown of T[±] to its formation as the basicity of amines increases.^{1,4–10}

As shown in Figure 2, the β_{nuc} value for the reactions of **1a**, **1c**, and **1e** with amines decreases from 0.65 to ca. 0.3–0.4. The change in the β_{nuc} value for the current reactions is much smaller than that reported for reactions which proceed through a stepwise mechanism with a change in the RDS. Besides, the β_{nuc} value of 0.65 is typical for reactions which have been

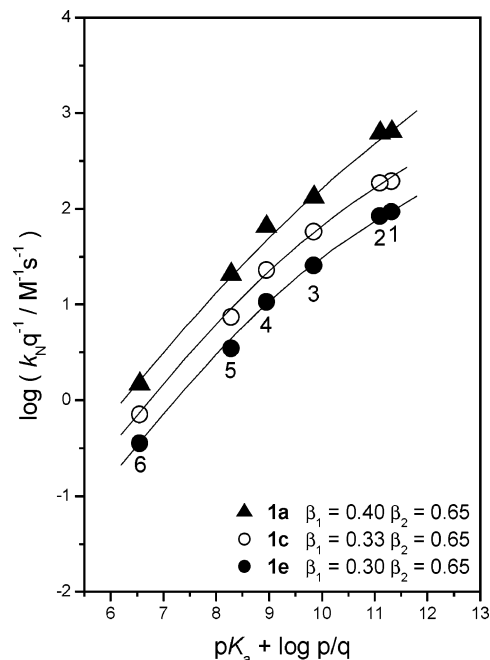


FIGURE 2. Brønsted-type plots for reactions of 2,4-dinitrophenyl X-substituted cinnamates with alicyclic secondary amines in 80 mol % H₂O/20 mol % DMSO at 25.0 ± 0.1 °C. The identity of points is given in Table 2.

suggested to proceed through a concerted mechanism.^{4–7} Thus, one can propose that the curved Brønsted-type plots shown in Figure 2 are not due to a change in the RDS but due to a change in the TS structure in accordance with a normal Hammond effect for a concerted mechanism, that is, an earlier TS for the reaction with a more reactive amine.²¹ A similar conclusion has been drawn for reactions of substituted benzoyl fluorides with primary amines. Song and Jencks have found curved Brønsted-type plots (β₂ = 0.67 at a low pK_a region and β₁ = 0.23 at a high pK_a region) and concluded that a normal Hammond effect is responsible for the curved Brønsted-type plots.²² Castro et al. have also concluded that reactions of bis(4-nitrophenyl) thionocarbonate and 2,4-dinitrophenyl 4-methylphenyl carbonate with secondary amines proceed through a concerted mechanism since the Brønsted-type plots obtained for these reactions exhibit only a small downward curvature (i.e., β₂ = ca. 0.5 and β₁ = 0.10).²³

To examine the above proposal, reactions of Y-substituted phenyl cinnamates (**3a–g**) and benzoates (**4a–g**) with piperidine and morpholine have been investigated. The effect of substituent Y in the leaving group on reactivity and mechanism is discussed in the following section.

Effect of a Leaving Group Substituent on Reactivity and Mechanism. Table 3 demonstrates that the reactivity of **3a–g** and **4a–g** decreases as the substituent Y in the leaving group becomes a weaker EWG. It is also shown that **3a–g** are more reactive than **4a–g** except for the reactions of **3a** and **4a** with piperidine. The effect of the substituent Y in the leaving group on reactivity is illustrated in Figure 3. The Brønsted-type plots for the reactions of **3a–g** and **4a–g** with piperidine are curved

(21) Hammond, G. S. *J. Am. Chem. Soc.* **1955**, *77*, 334–338.

(22) Song, B. D.; Jencks, W. P. *J. Am. Chem. Soc.* **1989**, *111*, 8479–8484.

(23) (a) Castro, E. A.; Santos, J. G.; Tellez, J.; Umana, M. I. *J. Org. Chem.* **1997**, *62*, 6568–6574. (b) Castro, E. A.; Andujar, M.; Campodonico, P.; Santos, J. G. *Int. J. Chem. Kinet.* **2002**, *34*, 309–315.

(20) Bell, R. P. *The Proton in Chemistry*; Methuen: London, U.K., 1959; p 159.

TABLE 3. Summary of Second-Order Rate Constants for Reactions of Y-Substituted Phenyl Cinnamates (**3a–g**) and Benzoates (**4a–g**, in Parenthesis) with Piperidine and Morpholine in 80 mol % H₂O/20 mol % DMSO at 25.0 ± 0.1 °C

	Y-PhOH	pK _a	k _N /M ⁻¹ s ⁻¹	
			piperidine	morpholine
a	Y = 3,4-(NO ₂) ₂	5.42	156 (191) ^a	13.2 (10.1)
b	Y = 4-NO ₂	7.14	12.3 (5.94) ^a	0.531 (0.0876) ^b
c	Y = 4-CHO	7.66	4.03 (0.852) ^a	0.0970 (0.00878)
d	Y = 4-COMe	8.05	1.71 (0.236) ^a	0.0296 (0.00299)
e	Y = 4-CO ₂ Et	8.50	1.24 (0.139)	0.0226 (0.00136)
f	Y = 3-Cl	9.02	0.297 (0.0159) ^a	0.00394 (–) ^c
g	Y = 3-COCH ₃	9.19	0.160 (0.00650) ^a	0.00160 (–) ^c

^a Data taken from ref 8b. ^b Data taken from ref 8f. ^c The reactivity was too low to determine rate constants.

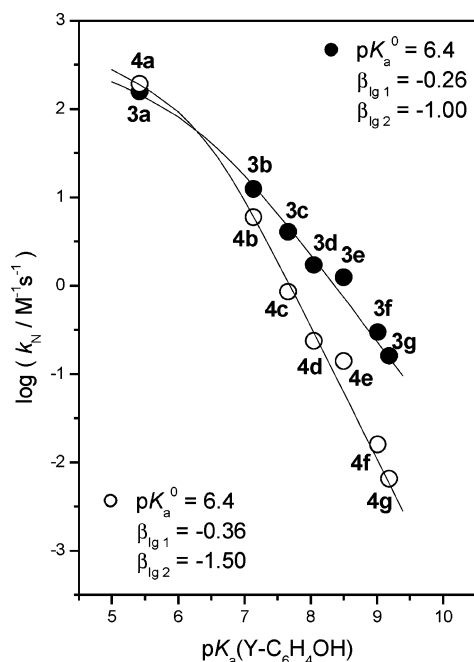


FIGURE 3. Brønsted-type plots for reactions of Y-substituted phenyl cinnamates (●; **3a–g**) and benzoates (○; **4a–g**) with piperidine in 80 mol % H₂O/20 mol % DMSO at 25.0 ± 0.1 °C. The identity of points is given in Table 3.

downwardly; that is, the β_{lg} value decreases from -1.00 to -0.26 and from -1.50 to -0.36 for the reactions of **3a–g** and **4a–g**, respectively.

Generally, the RDS of ester aminolysis has been reported to change from the breakdown of T[±] to its formation as the attacking amine becomes more basic than the leaving group or the leaving group becomes less basic than the amine by 4–5 pK_a units.^{1,4–10} The pK_a⁰, defined as the pK_a at the center of the Brønsted curvature, is 6.4 for the current reactions of **3a–g** and **4a–g** with piperidine, which is ca. 4.6 pK_a units smaller than the pK_a of the conjugate acid of piperidine (pK_a = 11.02). Thus, one might suggest that a change in the RDS is responsible for the nonlinear Brønsted-type plots in Figure 3 on the basis of the pK_a⁰ value. In fact, we have recently attributed the curved Brønsted-type plot for the reactions of **4a–g** with piperidine to

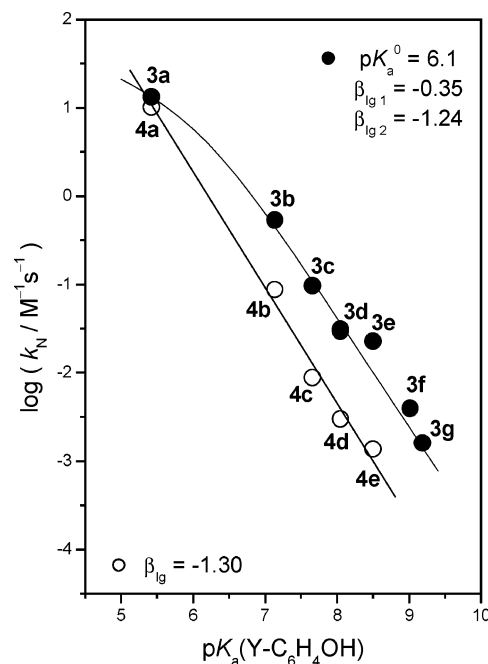


FIGURE 4. Brønsted-type plots for reactions of Y-substituted phenyl cinnamates (●; **3a–g**) and benzoates (○; **4a–e**) with morpholine in 80 mol % H₂O/20 mol % DMSO at 25.0 ± 0.1 °C. The identity of points is given in Table 3.

a change in the RDS.^{8b} However, for the reactions of **3a–g**, the decrease in the β_{lg} value from -1.00 to -0.26 is much smaller than that reported for reactions which proceed through a stepwise mechanism with a change in the RDS (e.g., from -1.50 to -0.36 for the reactions of **4a–g** with piperidine). Thus, one can suggest that the curved Brønsted-type plot for the reactions of **3a–g** with piperidine is not due to a change in the RDS.

To examine the above suggestion, Brønsted-type plots for the reactions of **3a–g** and **4a–e** with morpholine have been constructed. As shown in Figure 4, the Brønsted-type plot is linear for the reactions of **4a–e** but curved for those of **3a–g**. Since the pK_a of the conjugate acid of morpholine has been reported to be 8.65 in the current reaction medium, the pK_a⁰ should have been detected at the pK_a between 3.65 and 4.65 if the reactions of **3a–g** and **4a–e** with morpholine proceeded through a stepwise mechanism with a change in the RDS. As shown in Figure 4, the center of the Brønsted curvature for the reactions of **3a–g** with morpholine is 6.1, indicating that this curved Brønsted-type plot is clearly not due to a change in the RDS. Thus, one can conclude that the reactions of **3a–g** with piperidine and morpholine proceed through a concerted mechanism and the nonlinear Brønsted-type plots in Figures 3 and 4 are also due to a normal Hammond effect,²¹ that is, an earlier TS structure for a more reactive substrate.

Conclusions

The current study has allowed us to conclude the following: (1) The reactions of **1a–e** with amines result in much smaller ρ_X values but larger r values than those of **2a–e**. The larger r values found for the reactions of **1a–e** compared to those for the reactions of **2a–e** suggest that the presence of the $-\text{CH}=\text{CH}-$ bond in **1a–e** facilitates the ground-state resonance. (2) A distance effect and the nature of reaction mechanism (i.e., a

concerted mechanism for the reactions of **1a–e** have been suggested to be responsible for the small ρ_X values found for the reactions of **1a–e**. (3) The Brønsted-type plots for the reactions of **1a**, **1c**, and **1e** with alicyclic secondary amines exhibit a downward curvature; that is, the β_{nuc} value decreases from 0.65 to 0.3–0.4 as the basicity of amines increases. (4) The Brønsted-type plots for the reactions of **3a–g** with piperidine and morpholine are also curved, indicating that these curved Brønsted-type plots are not due to a change in the RDS but due to a normal Hammond effect for a concerted mechanism, that is, an earlier TS for a more reactive substrate.

Experimental Section

Materials. Y-Substituted phenyl X-substituted cinnamates (or benzoates) were readily prepared as reported²⁴ from the reactions of Y-substituted phenol and X-substituted cinnamoyl chloride under the presence of triethylamine in anhydrous ether and purified by column chromatography. Their purity was checked by their melting points for the known compounds, and the identity of unreported compounds (**1a**, **1b**, **1d**, **1e**, **3c**, **3e**, **3f**, and **3g**) was confirmed by elemental analysis and ¹H NMR spectra (Supporting Information). All unreported compounds gave good elemental analyses and ¹H NMR spectra. Amines and other chemicals used are of the highest quality available.

2,4-Dinitrophenyl 4-nitrocinnamate (1a): mp 170–172 °C; ¹H NMR (250 MHz, CDCl₃) δ 6.77–6.84 (d, $J = 17.5$ Hz, 1H), 7.59–7.62 (d, $J = 7.5$ Hz, 1H), 7.77–7.81 (d, $J = 10$ Hz, 2H), 7.96–8.03 (d, $J = 17.5$ Hz, 1H), 8.31–8.35 (d, $J = 10$ Hz, 2H), 8.57–8.61 (dd, $J_1 = 7.5$ Hz, $J_2 = 2.5$ Hz, 1H), 9.02–9.03 (d, $J = 2.5$ Hz, 1H). Anal. Calcd for C₁₅H₉N₃O₈: C, 50.15; H, 2.53. Found: C, 50.40; H, 2.75.

2,4-Dinitrophenyl 4-chlorocinnamate (1b): mp 139–140 °C; ¹H NMR (250 MHz, CDCl₃) δ 6.61–6.68 (d, $J = 17.5$ Hz, 1H), 7.42–7.46 (d, $J = 10$ Hz, 2H), 7.55–7.58 (d, $J = 7.5$ Hz, 1H), 7.57–7.61 (d, $J = 10$ Hz, 2H), 7.88–7.95 (d, $J = 17.5$ Hz, 1H), 8.55–8.59 (dd, $J_1 = 7.5$ Hz, $J_2 = 2.5$ Hz, 1H), 8.99–9.00 (d, $J = 2.5$ Hz, 1H). Anal. Calcd for C₁₅H₉ClN₂O₆: C, 51.67; H, 2.60. Found: C, 51.65; H, 2.67.

2,4-Dinitrophenyl 4-methylcinnamate (1d): mp 138–140 °C; ¹H NMR (250 MHz, CDCl₃) δ 6.59–6.65 (d, $J = 15$ Hz, 1H), 7.25–7.28 (d, $J = 7.5$ Hz, 2H), 7.51–7.54 (d, $J = 7.5$ Hz, 2H), 7.57–7.61 (d, $J = 10$ Hz, 1H), 7.91–7.97 (d, $J = 15$ Hz, 1H), 8.53–8.58 (dd, $J_1 = 10$ Hz, $J_2 = 2.5$ Hz, 1H), 8.98–8.99 (d, $J = 2.5$ Hz, 1H). Anal. Calcd for C₁₆H₁₂N₂O₆: C, 58.54; H, 3.68. Found: C, 58.49; H, 3.70.

2,4-Dinitrophenyl 4-methoxycinnamate (1e): mp 132–134 °C; ¹H NMR (250 MHz, CDCl₃) δ 6.49–6.55 (d, $J = 15$ Hz, 1H), 6.95–7.00 (dd, $J_1 = 10$ Hz, $J_2 = 2.5$ Hz, 2H), 7.57–7.61 (d, $J = 10$ Hz, 1H), 7.65–7.68 (d, $J = 7.5$ Hz, 1H), 7.89–7.95 (d, $J = 15$ Hz, 1H), 8.53–8.57 (dd, $J_1 = 7.5$ Hz, $J_2 = 2.5$ Hz, 1H), 8.97–8.98 (d, $J = 2.5$ Hz, 1H). Anal. Calcd for C₁₆H₁₂N₂O₇: C, 55.82; H, 3.51. Found: C, 55.81; H, 3.53.

4-Formylphenyl cinnamate (3c): mp 82–85 °C; ¹H NMR (250 MHz, CDCl₃) δ 6.61–6.67 (d, $J = 15$ Hz, 1H), 7.36–7.39 (d, $J = 7.5$ Hz, 2H), 7.43–7.48 (m, 3H), 7.59–7.63 (dd, $J_1 = 7.5$ Hz, $J_2 = 2.5$ Hz, 2H), 7.88–7.94 (d, $J = 15$ Hz, 1H), 7.95–7.98 (d, $J = 7.5$ Hz, 2H), 10.0 (s, 1H). Anal. Calcd for C₁₆H₁₂O₃: C, 76.18; H, 4.79. Found: C, 75.84; H, 4.75.

4-(Ethoxycarbonyl)phenyl cinnamate (3e): mp 89–91 °C; ¹H NMR (250 MHz, CDCl₃) δ 1.37–1.43 (t, $J = 7.5$ Hz, 3H), 4.35–

4.43 (q, $J = 7.5$ Hz, 2H), 6.60–6.67 (d, $J = 17.5$ Hz, 1H), 7.24–7.28 (d, $J = 10$ Hz, 2H), 7.43–7.45 (m, 3H), 7.58–7.62 (dd, $J_1 = 7.5$ Hz, $J_2 = 2.5$ Hz, 2H), 7.86–7.93 (d, $J = 17.5$ Hz, 1H), 8.10–8.14 (d, $J = 10$ Hz, 2H). Anal. Calcd for C₁₈H₁₆O₄: C, 72.96; H, 5.44. Found: C, 72.98; H, 5.45.

3-Chlorophenyl cinnamate (3f): mp 62–64 °C; ¹H NMR (250 MHz, CDCl₃) δ 6.58–6.65 (d, $J = 17.5$ Hz, 1H), 7.10–7.11 (m, 1H), 7.21–7.23 (m, 1H), 7.25–7.26 (m, 1H), 7.31–7.37 (t, $J = 7.5$ Hz, 1H), 7.42–7.45 (m, 3H), 7.58–7.62 (dd, $J_1 = 7.5$ Hz, $J_2 = 2.5$ Hz, 2H), 7.84–7.91 (d, $J = 17.5$ Hz, 1H). Anal. Calcd for C₁₅H₁₁ClO₂: C, 69.64; H, 4.29. Found: C, 69.67; H, 4.30.

3-Acetylphenyl cinnamate (3g): mp 69–71 °C; ¹H NMR (250 MHz, CDCl₃) δ 2.62–2.65 (s, 3H), 6.62–6.68 (d, $J = 15$ Hz, 1H), 7.38–7.41 (m, 1H), 7.42–7.46 (m, 3H), 7.49–7.55 (t, $J = 7.5$ Hz, 1H), 7.59–7.63 (dd, $J_1 = 7.5$ Hz, $J_2 = 2.5$ Hz, 2H), 7.76–7.77 (m, 1H), 7.84–7.87 (d, $J = 15$ Hz, 1H), 7.93 (s, 1H). Anal. Calcd for C₁₇H₁₄O₃: C, 76.68; H, 5.30. Found: C, 76.51; H, 5.31.

Kinetics. The kinetic study was performed with a UV–vis spectrophotometer for slow reactions ($t_{1/2} > 10$ s) or a stopped-flow spectrophotometer for fast reactions ($t_{1/2} \leq 10$ s) equipped with a constant temperature circulating bath. The reactions were followed by monitoring the appearance of Y-substituted phenoxide at a fixed wavelength corresponding to the λ_{max} . Due to the low solubility of the substrates in pure water, aqueous DMSO (80 mol % H₂O/20 mol % DMSO) was used as the reaction medium. Doubly glass distilled water was further boiled and cooled under nitrogen just before use.

All of the reactions were carried out under pseudo-first-order conditions in the presence of excess amines. Typically, the reaction was initiated by adding 5 μ L of a 0.01 M of substrate solution in MeCN by a 10 μ L gastight syringe to a 10 mm quartz UV cell containing 2.50 mL of the thermostated reaction mixture made up of solvent and an aliquot of amine stock solution. The stock solution of amines (ca. 0.2 M) was prepared in a 25.0 mL volumetric flask under nitrogen by adding 2 equiv of amines and 1 equiv of standardized HCl solution to obtain a self-buffered solution. All of the solutions were transferred by gastight syringes under nitrogen. Generally, the concentration of amines was varied over the range of $(1-100) \times 10^{-3}$ M, while the substrate concentration was 2×10^{-5} M. The plots of $\ln(A_{\infty} - A_t)$ versus time were linear over ca. 90% of the total reaction. Usually, five different concentrations of amines were used to determine the k_N value from the slope of the linear plot of k_{obsd} versus amine concentration.

Product Analysis. Y-Substituted phenoxide was liberated quantitatively and identified as one of the reaction products by comparison of the UV–vis spectra after the completion of the reactions with those of the authentic samples under the same reaction conditions.

Acknowledgment. This work was supported by a grant from KOSEF of Korea (R01-2004-000-10279-0).

Supporting Information Available: Figure S1 for Hammett plots for the reactions of **1a–e** with piperidine, morpholine, and piperazinium ion. ¹H NMR spectra for **1a**, **1b**, **1d**, **1e**, **3c**, **3e**, **3f**, and **3g**, Tables S1–S24 for the kinetic data for reactions of **1a–e** with secondary amines, Tables S25–S38 for the kinetic data for reactions of **3a–g** with secondary amines, Table S39 for the kinetic data for reactions of **4e** with piperidine, and Tables S40–S43 for the kinetic data for reactions of **4a**, **4c**, **4d**, and **4e** with morpholine. This material is available free of charge via the Internet at <http://pubs.acs.org>.

JO0705061

(24) (a) Womack, E. B.; McWhirter, J. *Org. Synth.* **1940**, *20*, 77. (b) Suh, J.; Lee, B. H. *J. Org. Chem.* **1980**, *45*, 3103–3107.